https://doi.org/10.15407/ujpe68.2.92

O.A. BURYI,[1] D.M. VYNNYK,[1] T.I. VORONIAK,[2] I.V. STASYSHYN,[1,2]
A.T. RATYCH,[1] A.S. ANDRUSHCHAK [1]

[1] Lviv Polytechnic National University
(12, S. Bandery Str., Lviv 79013, Ukraine)
[2] G.V. Karpenko Physico-Mechanical Institute, Nat. Acad. of Sci. of Ukraine
(5, Naukova Str., Lviv 79601, Ukraine)

PROPAGATION OF ACOUSTIC WAVES IN CALCIUM TUNGSTATE CRYSTALS

On the basis of the solution of Christoffel equation, the phase-velocity surfaces for a quasi-longitudinal acoustic wave (AW) and the fast and slow quasi-transverse AWs in the $CaWO_4$ crystals have been plotted, and the extreme velocity value for each AW type and the direction of its realization have been determined. It is shown that the maximum shear angle occurs for the AW propagating in the (001) plane; in the case, the shear angle can reach a value of about 45° for the quasi-transverse AW, and about 18° for the quasi-longitudinal one. The quadratic anisotropy coefficients W_1 and W_2 for various AW propagation directions are determined. It is shown that there exist such directions of the quasi-transverse AW propagation in the $CaWO_4$ crystal for which the divergence (the quadratic anisotropy coefficient $|W_2|$) significantly exceeds the divergence that would occur in the case of isotropic medium. A direction in which the crystal anisotropy induces an additional focusing of the acoustic beam of the slow quasi-transverse AW or an additional divergence of the acoustic beam of the fast quasi-transverse AW is determined. The experimental values of the velocities and shear angles of the AWs are presented, which confirm the reliability of the obtained calculation results.

K e y w o r d s: acoustic wave, Christoffel equation, acoustic wave shear.

1. Introduction

Crystals of calcium tungstate $CaWO_4$ with the scheelite structure (the symmetry class 4/m) are a well-known material for applications in the scintillation [1, 2] and luminescence [3, 4] dosimetry, optoelectronic devices [5, 6], and lasers [7, 8]. At the same time, on the basis of the studies of the piezoelectric, elasto-optical, and acousto-optical characteristics of $CaWO_4$ crystals, which were performed in works [9, 10], a conclusion can be drawn that this material is promising for its application in acousto-optical devices, in particular, operating in the ultraviolet spectral range (up to 130 nm). For instance, according for the estimate made in work [9], the value of the acousto-optical figure-of-merit for this material is $M_2 = 14.0 \times 10^{-15}$ s^3/kg, which is comparable with the theoretically achievable maximum value $M_2 = 15.9 \times 10^{-15}$ s^3/kg for lithium niobate and is almost an order of magnitude higher than the M_2-value for quartz.

When designing acousto-optical devices, also important are the material properties governing the propagation of acoustic waves (AWs) in this material. In particular, these are the propagation velocities of acoustic waves with various polarizations, the values of wave attenuation and shear angle, the diffraction divergence of an acoustic beam, and so forth. When analyzing the processes of the AW propagation in anisotropic media, it should be taken into account that the diffraction divergence of acoustic beam in them can be stronger than the divergence in an isotropic medium. For instance, the divergence of an acoustic beam in the paratellurite crystal TeO_2 is 60 times as large as the diffraction limit [11]. It is also known that the shear angles of AWs can reach tens of degrees for a lot of crystals [12], and this fact

C i t a t i o n: Buryi O.A., Vynnyk D.M., Voroniak T.I., Stasyshyn I.V., Ratych A.T., Andrushchak A.S. Propagation of acoustic waves in calcium tungstate crystals. *Ukr. J. Phys.* **68**, No. 2, 92 (2023). https://doi.org/10.15407/ujpe68.2.92.
Ц и т у в а н н я: Бурий О.А., Винник Д.М., Вороняк Т.I., Стасишин I.В., Ратич А.Т., Андрущак А.С. Розповсюдження акустичних хвиль у кристалах вольфрамату кальцiю. *Укр. фiз. журн.* **68**, №2, 92 (2023).

must be taken into account, as well when designing an acousto-optical device.

However, a detailed analysis of the features of the AW propagation has not been carried out yet for $CaWO_4$ crystals (the calculations made in work [9] included the determination of the velocities and shear angles, but they did not have a general nature from the viewpoint of describing the acoustic properties of the crystal). Therefore, in this work, we theoretically calculated the propagation velocities of acoustic waves, their shear angles, and diffraction divergence in $CaWO_4$ crystals. To confirm the calculation results, we also carried out experimental measurements of the AW velocities and shear angles for the principal crystallographic directions in those crystals.

2. Theoretical Study of the Features of Acoustic Wave Propagation and Their Analysis

Our analysis of the features of the AW propagation in $CaWO_4$ crystals is based on the Christoffel equation, which determines the acoustic wave velocity and unit polarization vectors of this wave, $\mathbf{f}_q$, for each direction of its wave normal $\mathbf{a}$ [12]:

$$(\mathbf{a}\hat{c}\mathbf{a})\mathbf{f}_q = \rho {V_q}^2 \mathbf{f}_q. \tag{1}$$

Here, ρ is the material density, V is the AW velocity, and $\hat{c}$ is the elasticity tensor. The non-zero components of the latter are as follows (in 10^{11} Pa units): $c_{11} = = c_{22} = 1.43$, $c_{12} = 0.554$, $c_{13} = c_{23} = 0.504$, $c_{16} = = -c_{26} = 0.221$, $c_{33} = 1.28$, $c_{44} = c_{55} = 0.340$, and $c_{66} = 0.449$, as well as those obtained by permuting the subscripts [13]. The AW shear angle γ_a is calculated according for the formula [12]

$$\cos \gamma_a = \frac{\mathbf{au}}{|\mathbf{u}|}, \tag{2}$$

where

$$\mathbf{u} = \frac{\mathbf{f}_q \hat{c} \mathbf{f}_q \mathbf{a}}{\rho V_q} \tag{3}$$

is the velocity vector of the elastic wave along the beam.

2.1. Propagation velocities of acoustic waves

The spatial distribution of acoustic wave velocities V can be represented in the form of phase-velocity surfaces [12]. The latter are plotted as surfaces for which the direction of the radius vector of each point corresponds to the AW propagation direction, and the magnitude of this radius vector is equal to the corresponding phase velocity. For the sake of consideration generality, it is necessary to consider three polarization states of the waves propagating in each direction: quasi-longitudinal (QL), fast quasi-transverse (OTF), and slow quasi-transverse (OTS) acoustic waves. The phase-velocity surfaces for the $CaWO_4$ crystal were calculated on the basis of the Christoffel equation (1), and they are exhibited in Table 1.

Table 1 also demonstrates the maximum and minimum velocities for each type of the acoustic wave polarization and (in parentheses) the values of the angles θ_a and ϕ_a describing the corresponding direction of acoustic wave propagation in the spherical coordinate system. Since the symmetry of the phase-velocity surface corresponds to the crystal symmetry (4/m), only the angle values for one direction are presented, whereas the others can be determined by using the appropriate symmetry operations. Table 2 contains the calculated values of phase velocities for AWs with various polarizations and for some selected directions of their propagation.

2.2. Tilt angles of acoustic waves

The surfaces of the shear angles γ of acoustic waves were plotted analogously to the phase-velocity surfaces. The maximum shear angles, as well as the values of the angles θ_γ and ϕ_γ that determine the corresponding direction of acoustic wave propagation in the spherical coordinate system are given in parentheses in Table 3. The presented data testify that the maximum shear of the acoustic wave takes place at its propagation in the (001) plane. In this case, the shear angle can reach a value of approximately 45° for quasi-transverse AWs. At the same time, this quantity is substantially smaller for the quasi-longitudinal wave, although it remains significant by magnitude (about 18°).

The cross-sections of the surfaces exhibited in Table 3 by the (001) plane are shown in Fig. 1. The values of the shear angles for some selected directions of AW propagation are given in Table 4.

2.3. Acoustic wave divergence

It is known that the anisotropy of the medium, where an acoustic beam propagates, can induce a substan-

Table 1. **Phase-velocity surfaces and their extreme values for waves with various polarizations in $CaWO_4$ crystals**

Wave type	Surface (isometry and top view)	$V_{\max}$, m/s, θ_a, ϕ_a, deg	$V_{\min}$, m/s, θ_a, ϕ_a, deg
QL	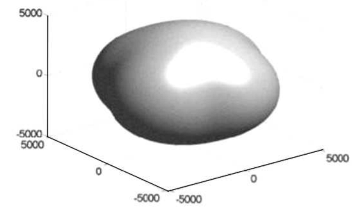 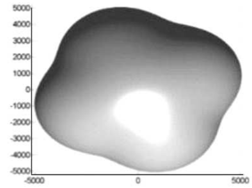	5227 (90; 22)	4462 (60; 68)
OTF	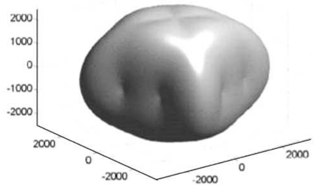 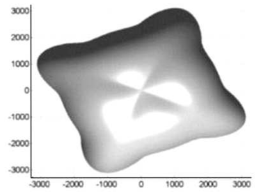	3311 (90; 68)	2368 (0; 0) and (90; 60)
OTS	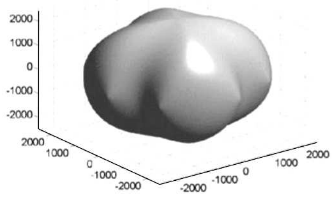 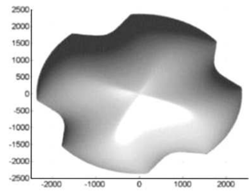	2475 (46; 68)	1917 (90; 22)

Table 2. **Phase-velocity surfaces and their extreme values for waves with various polarizations in $CaWO_4$ crystals**

Wave type	Directions				
	[001]	[100]	[110]	[101]	[111]
QL	4595	4937	4954	4593	4598
OTF	2368	2574	2541	2820	2818
OTS	2368	2368	2368	2329	2321

tial diffraction divergence of the beam in comparison with that taking place in the isotropic medium [11, 14]. At the qualitative level, the influence of anisotropy on the beam divergence is determined using the quadratic anisotropy coefficients $W_{1,2} = K_{1,2}/V_q$, where $K_{1,2}$ are the eigenvalues of the planar tensor $\hat{K} = \partial\mathbf{u}/\partial\mathbf{a}$ (one of the three eigenvalues of this tensor is always zero, so only two anisotropy coefficients, W_1 and W_2, are considered [14]). By their physical sense, the absolute values of W_1 and W_2 show how much the diffraction divergence of the beams propagating in the directions of the principal anisotropy axes is larger than the divergence in an isotropic medium.

According to the results of work [14], the components of the tensor $\hat{K}$ are calculated as follows:

$$K_{ik} = -B^{-1}(B_{ik} - B_i u_k - u_i B_k + B' u_i u_k). \qquad (4)$$

Here, u_i are the components of the beam velocity vector, and the other quantities are determined as follows:

$$B = 2V_q(3V_q^4 - 2V_q^2\Gamma_{\mathrm{I}} + \Gamma_{\mathrm{II}}), \qquad (5)$$

$$B' = 2V_q(15V_q^4 - 6V_q^2\Gamma_{\mathrm{I}} + \Gamma_{\mathrm{II}}), \qquad (6)$$

Table 3. **Tilt-angle surfaces and their maximum values for waves with various polarizations in $CaWO_4$ crystals**

Wave type	Surface (isometry and top view)		$\gamma_{\max}$, m/s, θ_γ, ϕ_γ, deg
QL	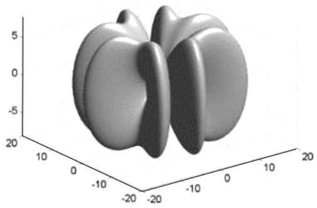	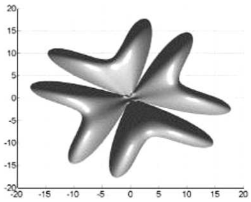	17.9 (90; 54)
OTF	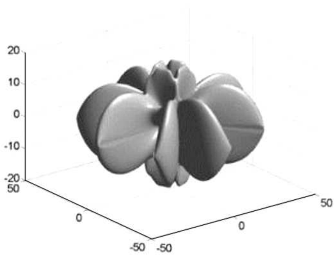	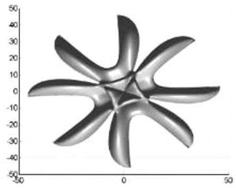	45.9 (90; 42)
OTS	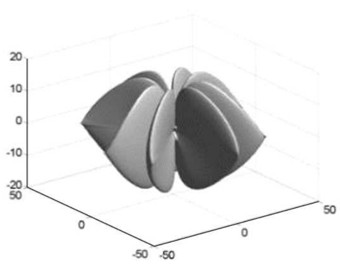	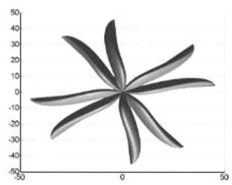	45.5 (90; 40)

Table 4. **AW shear angles (in degrees) for some directions in $CaWO_4$ crystals**

Wave type	Directions				
	[001]	[100]	[110]	[101]	[111]
QL	0	15.4°	15.1°	8.9°	9.0°
OTF	0	45.4°	45.6°	6.0°	5.5°
OTS	0	0	0	21.6°	21.8°

$$B_i = 2V_q\left(2V_q^2\frac{\partial\Gamma_{\mathrm{I}}}{\partial a_i} - \frac{\partial\Gamma_{\mathrm{II}}}{\partial a_i}\right), \tag{7}$$

$$B_{ik} = -V_q^4\frac{\partial^2\Gamma_{\mathrm{I}}}{\partial a_i\partial a_k} + V_q^2\frac{\partial^2\Gamma_{\mathrm{II}}}{\partial a_i\partial a_k} - \frac{\partial^2\Gamma_{\mathrm{III}}}{\partial a_i\partial a_k}. \tag{8}$$

where Γ_{I}, Γ_{II}, and Γ_{III} are the first, second, and third, respectively, invariants of the tensor

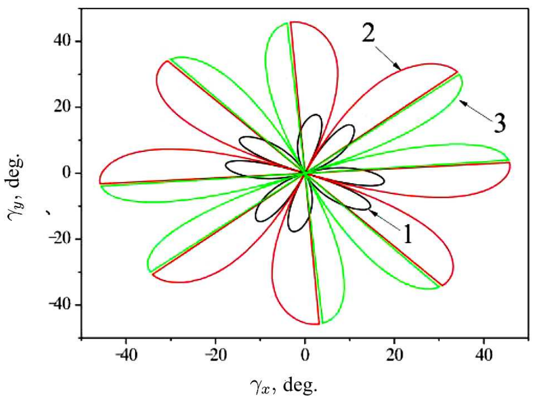

Fig. 1. Cross-sections of the surfaces representing the spatial distribution of the shear angle by the (001) plane for various AWs: the quasi-longitudinal AW (*1*), the fast quasi-transverse AW (*2*), and the slow quasi-transverse AW (*3*)

Table 5. **Surfaces of the quadratic anisotropy coefficients for waves of various polarizations in $CaWO_4$ crystal**

Wave type	$\|W_1\|$	$\|W_2\|$
QL	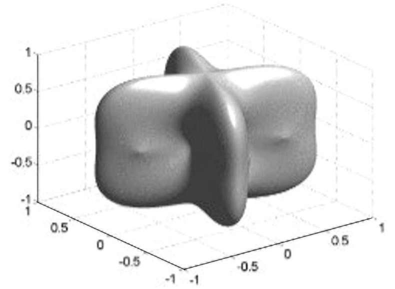 Maximum: 1.1 ($\theta = 49.5°$; $\phi = 68°$) Minimum: 0.26 ($\theta = 89.5°$; $\phi = 23°$)	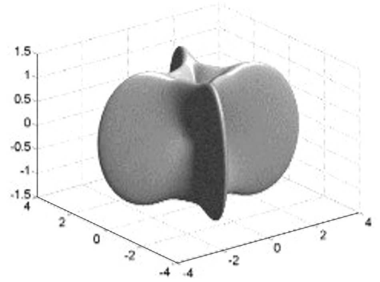 Maximum: 3.6 ($\theta = 90°$; $\phi = 68°$) Minimum: 0.53 ($\theta = 90°$; $\phi = 22.5°$)
OTF	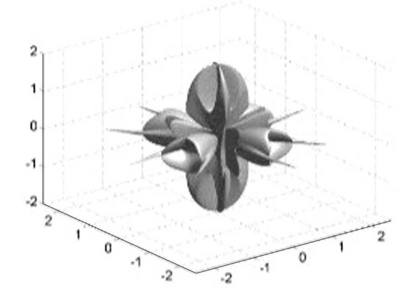 Maximum: 2.4 ($\theta = 90°$; $\phi = 4{,}5°$) Minimum: 3.2×10^{-5} ($\theta = 32°$; $\phi = 9.5°$)	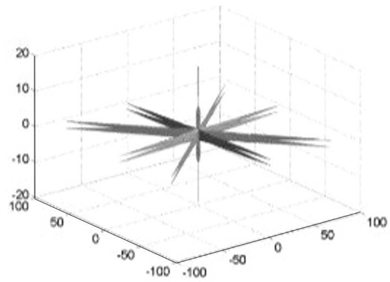 Maximum: 116.1 ($\theta = 89.5°$; $\phi = 41°$) Minimum: 0.78 ($\theta = 51.5°$; $\phi = 68°$)
OTS	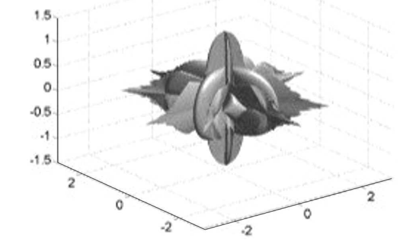 Maximum: 2.7 ($\theta = 90°$; $\phi = 6°$) Minimum: 7.8 $\times 10^{-5}$ ($\theta = 10°$; $\phi = 56.5°$)	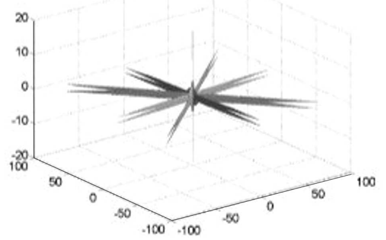 Maximum: 113.1 ($\theta = 89.5°$; $\phi = 41°$) Minimum: 0.65 ($\theta = 46°$; $\phi = 68°$)

$\Gamma_{ik} = \rho^{-1} c_{ijkl}\, a_j a_l$; and c_{ijkl} are the components of the elastic modulus tensor in the four-index notation.

The absolute values of the quadratic anisotropy coefficients W_1 and W_2 were determined for various directions of acoustic wave propagation in the $CaWO_4$ crystal, and they are quoted in Table 5 (for the sake of definiteness, it was assumed in calculations that the inequality $|W_2| > |W_1|$ always holds). Figure 2 demonstrates the cross-sections of the surfaces presented in Table 5 by the (001) plane.

As one can see from Table 5 and Fig. 2, there are such propagation directions of quasi-transverse AWs in the $CaWO_4$ crystal for which the divergence (the quadratic anisotropy coefficient $|W_2|$) substantially exceeds the value that would occur, if the medium were isotropic. For both types of quasi-transverse AWs (fast and slow), those directions coincide ($\theta = 89.5°$ and $\phi = 41°$, see Table 5). At the same time, they do not correspond to the directions of the axes of the crystallophysical coordinate system. For

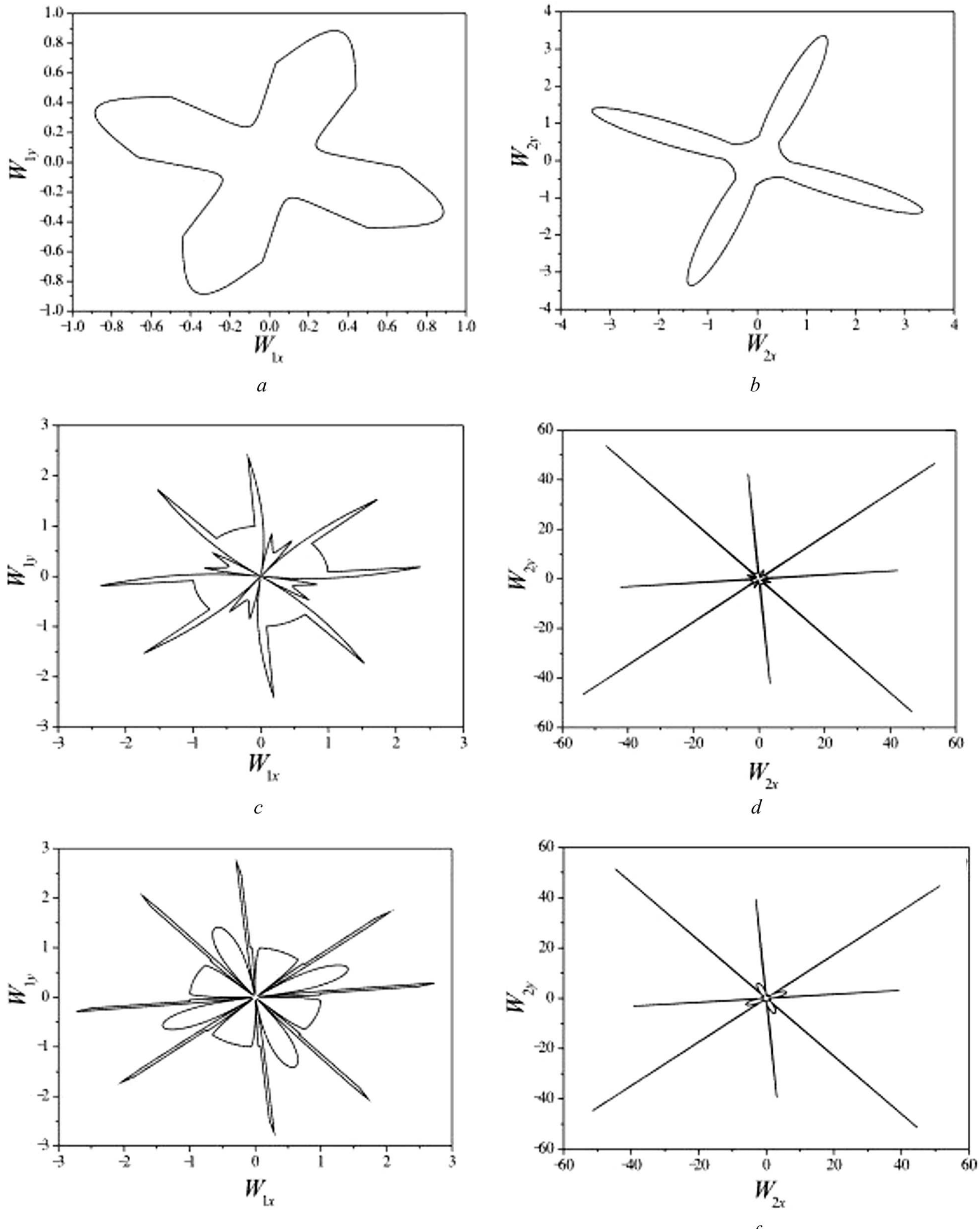

Fig. 2. Cross-sections of the surfaces of quadratic coefficients W_1 and W_2 (see Table 5) by the (001) plane: for the quasi-longitudinal AW (*a, b*), for the fast quasi-transverse AW (*c, d*), for the slow quasi-transverse AW (*e, f*)

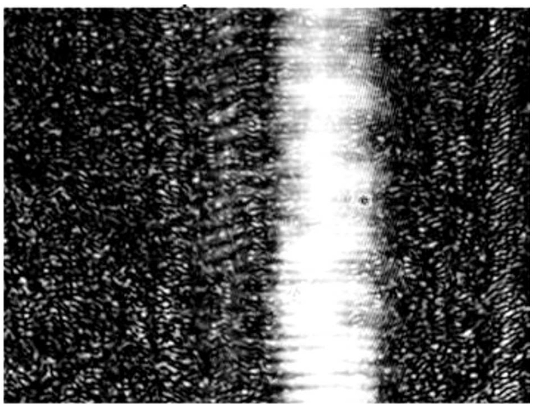

a

b

Fig. 3. Examples of visualization of acoustic waves in the studied specimens: for a longitudinal wave propagating in the [001] direction (*a*), for a longitudinal wave propagating in the [100] direction (*b*)

Table 6. **Experimentally determined velocities of acoustic waves (m/s) for some directions in $CaWO_4$ crystals**

Wave type	Directions		
	[001]	[100]	[110]
Longitudinal wave	4366	4856	4867
Transverse wave (OTS polarization)	2231	2222	2328

quasi-transverse AWs propagating in the (001) plane, the indicated large discrepancy (see Fig. 2, *d* and Fig. 2, *f*) takes place in the planes that are perpendicular to (001). However, an important difference consists in that the quadratic coefficients W_2 for the fast and slow quasi-transverse AWs differ in sign at the point, where $|W_2|$ is maximum; namely, $W_2 > 0$ for the fast AW, and $W_2 < 0$ for the slow one. The negative sign of W_2 in the latter case means that the crystal anisotropy causes an additional focusing of the slow quasi-transverse AW and a divergence of the fast quasi-transverse one at their propagation in this direction.

3. Experimental Results for the Velocities and Tilt Angles of Acoustic Wave Propagation

For experimental studies, specimens of $CaWO_4$ crystals with straight cuts were prepared. The parallelism of the specimen faces was 10°. When mechanically processing (grinding and polishing) the specimens, their interferometric control was carried out according to the technology described in work [15].

3.1. Experimental study of sound velocities

The sound velocity in the studied crystals was measured using the Papadakis method [16]. We used piezoelectric transducers made of the $LiNbO_3$ crystal of $Y + 36°$ cut for the excitation of longitudinal acoustic waves, and piezoelectric transducers made of the same crystal of $Y + 163°$ cut for the excitation of transverse waves.

The measured values of the acoustic wave velocities are given in Table 6. As follows from their comparison with the values given in Tables 2 and 5, the experimental and theoretical results obtained for the acoustic wave velocities coincide with an accuracy not worse than 6%.

3.2. Experimental study of acoustic wave shear angles

The experimental study of the shear angles of acoustic waves was carried out in the framework of the shadow method (the Tepler method) [9]. In the course of experiments, the acoustic beam was initially generated in a buffer (a Bragg cell), the light and sound conductor of which was made of fused SiO_2. A researched specimen was attached to the free face of this light and sound conductor using a special glue. The acoustic beam, when having reached the free face of the buffer, was partially reflected from it, but it also partially passed into the specimen. The acoustic beams

Table 7. **Experimentally determined shear angles for some directions in $CaWO_4$ crystals**

Wave type	Directions		
	[001]	[100]	[110]
Longitudinal	0	15.1°	15.1°
Transverse	0	0	0

in the buffer and the specimen were visualized with the help of an extended parallel laser beam that had diffracted at the acoustic beams. The frequency of a transverse AW was 150 MHz (this was the central frequency of the matched piezoelectric transducer of the applied buffer). In order to register the diffracted laser beam (see Fig. 3), a digital CCD camera was applied. In the buffer, the acoustic beam propagated along the normal to the free face of the light and sound guide.

The study was carried out making use of three specimens. The average values of the experimentally determined shear angles are quoted in Table 7. As one can see, the results of experimentally found shear angles are in full agreement with the calculated data.

4. Conclusions

By solving the Christoffel equation, the phase-velocity surfaces for the quasi-longitudinal, fast quasi-transverse, and slow quasi-transverse AWs in the $CaWO_4$ crystal are plotted, and the extreme velocity values, as well as the directions in which they are realized, are determined for each AW type. It is shown that the maximum and minimum velocities of the quasi-longitudinal AW are equal to 5227 and 4462 m/s, respectively; the corresponding values are equal to 3311 and 2368 m/s, respectively, for the fast quasi-transverse AW, and to 2475 and 1917 m/s, respectively, for the slow quasi-transverse AW. The AW shear is maximum, if the wave propagates in the (001) plane; in this case, the shear angle can reach a value of about 45° for the quasi-transverse AWs, and about 18° for the quasi-longitudinal AW.

The quadratic coefficients of anisotropy W_1 and W_2 in $CaWO_4$ crystals are determined for all three types of AWs and various directions of their propagation. It is shown that there exist such propagation directions of quasi-transverse AWs in this crystal for which the divergence (the quadratic anisotropy coefficient $|W_2|$) is substantially larger than the divergence that would occur in the isotropic medium case. The maximum of $|W_2|$ is equal to about 116 for the fast quasi-transverse AW, and about 113 for the slow quasi-transverse AW; in both cases, it takes place in the same direction determined by the angles $\theta = 89.5°$ and $\phi = 41°$ in the spherical coordinate system and the associated symmetry elements of the class 4/m. It is shown that the maxima of the quadratic coefficients W_2 for the fast and slow quasi-transverse AWs are opposite in sign: $W_2 > 0$ for the fast AW, and $W_2 < 0$ for the slow one. This fact means that the crystal anisotropy causes an additional focusing of the acoustic beam of the slow quasi-transverse AW and, on the contrary, an additional divergence of the acoustic beam of the fast quasi-transverse AW in the indicated direction.

The experimental results obtained for the velocities and shear angles of all three types of acoustic waves are reported. Within the experimental accuracy, they coincide with the corresponding calculated values, which confirms the reliability of the latter.

1. M.V. Sivers, M. Clark, P.C.F. Di Stefano, A. Erb, A. Gütlein, J.-C. Lanfranchi, A. Münster, P. Nadeau, M. Piquemal, W. Potzel, S. Roth, K. Schreiner, R. Strauss, S. Wawoczny, M. Willers, A. Zöller. Low-temperature scintillation properties of $CaWO_4$ crystals for rareevent searches. *J. Appl. Phys.* **118**, 164505 (2015).
2. A. Phuruangrata, T. Thongtemb, S. Thongtema. Synthesis, characterisation and photoluminescence of nanocrystalline calcium tungstate. *J. Exper. Nanosci.* **5**, 263 (2010).
3. A. Shmilevich, D. Weiss, R. Chen, N. Kristianpoller. Phototransferred thermoluminescence of $CaWO_4$ crystals. *Radiation Protection Dosimetry* **84**, 131 (1999).
4. C. Michail, I. Valais, G. Fountos, A. Bakas, C. Fountzoula, N. Kalyvas, A. Karabotsos, I.A. Sianoudis, I. Kandarakis. Luminescence efficiency of calcium tungstate ($CaWO_4$) under X-ray radiation: Comparison with $Gd_2O_2S:Tb$. *Measurement* **120**, 213 (2018).
5. F.B. Xiong, H.F. Lin, L.J. Wang, H.X. Shen, Y.P. Wang, W.Z Zhu. Luminescent properties of red-light-emitting phosphors $CaWO_4:Eu^{3+}$, Li^+ for near UV LED. *Bull. Mater. Sci.* **38**, 1 (2015).
6. H.P. Barbosa, .I.G.N. Silva, C.M.F.C. Felinto, E.E.S. Teotonio, O.L. Malta, H.F. Brito. Photoluminescence of single-phased white light emission materials based on simultaneous Tb^{3+} , Eu^{3+} and Dy^{3+} doping in $CaWO_4$ matrix. *J. Alloy. Compd.* **696**, 820 (2017).
7. N. Faure, C. Borel, M. Couchaud, G. Basset, R. Templier, C. Wyon. Optical properties and laser performance of neodymium doped scheelites $CaWO_4$ and $NaGd(WO_4)_2$. *Appl. Phys. B* **63**, 593 (1996).

8. J. Chen, L. Dong, F. Liu, H. Xu, J. Liu. Investigation of Yb : $CaWO_4$ as a potential new self-Raman laser crystal. *Cryst. Eng. Comm.* **23**, 427 (2021).
9. A.S. Andrushchak, O.A. Buryy, N.M. Demyanyshyn, Z.Yu. Hotra, B.G. Mytsyk. Global maxima of the acousto-optic effect in $CaWO_4$ crystals. *Acta Phys. Pol. A* **133**, 928 (2018).
10. B.G. Mytsyk, Ya.P. Kost, N.M. Demyanyshyn, A.S. Andrushchak, I.M. Solskii. Piezooptical coefficients of $CaWO_4$ crystals. *Crystallogr. Rep.* **60**, 130 (2015).
11. J.S. Kastelik, M.J. Gazalet, C. Bruneel, E. Bridox. Acoustic shear wave propagation in paratellurite with reduced spreading. *J. Appl. Phys.* **74**, 2813 (1993).
12. Yu. Sirotin, M. Shaskolskaja. *Fundamentals of Crystal Physics* (Mir Publishers, 1983).
13. J.M. Farley, G.A. Saunders. The elastic constants of $CaWO_4$. *Solid State Commum.* **9**, 965 (1971).
14. A.G. Khatkevich. Diffraction and propagation of ultrasonic radiation beams in single crystals. *Akust. Zh.* **24**, 108 (1978) (in Russian).
15. A.S. Andrushchak, T.I. Voronyak, O.V. Yurkevych, N.A. Andrushchak, A.V. Kityk. Interferometric technique for controlling wedge angle and surface flatness of optical slabs. *Opt Laser Eng.* **51**, 342 (2013).
16. E.P. Papadakis. Ultrasonic phase velocity by the pulse-echo overlap method incorporating diffraction phase correction. *J. Acoust. Soc. Am.* **42**, 1045 (1967).
17. S. Kino. *Acoustic Waves* (Prentice Hall, 1987).

Received 14.09.21.
Translated from Ukrainian by O.I. Voitenko

О.А. Бурий, Д.М. Винник, Т.І. Вороняк,
І.В. Стасишин, А.Т. Ратич, А.С. Андрущак

РОЗПОВСЮДЖЕННЯ АКУСТИЧНИХ ХВИЛЬ У КРИСТАЛАХ ВОЛЬФРАМАТУ КАЛЬЦІЮ

На основі розв'язку рівняння Кристоффеля побудовано поверхні фазових швидкостей для квазіпоздовжньої, квазіпоперечної швидкої та квазіпоперечної повільної акустичних хвиль (АХ) у кристалі $CaWO_4$, визначено екстремальні значення швидкості для кожного типу АХ та напрямки, в яких вони реалізуються. Показано, що максимальне знесення АХ відбувається під час її розповсюдження в площині (001), при цьому для квазипоперечних АХ значення кута знесення може досягати величини близько 45°, а для квазипоздовжньої – близько 18°. Визначено квадратичні коефіцієнти анізотропії W_1 та W_2 для різних напрямків розповсюдження АХ. Показано, що в кристалі існують такі напрямки поширення квазипоперечних АХ, для яких розбіжність (квадратичний коефіцієнт анізотропії $|W_2|$) значно перевищує ту, яка мала б місце у випадку ізотропного середовища. Визначено напрям, в якому під час поширення квазипоперечної повільної АХ анізотропія спричиняє додаткове фокусування акустичного пучка, тоді як для квазипоперечної швидкої АХ, навпаки, – додаткову розбіжність. Наведено результати експериментальних значень швидкостей та кутів знесення АХ, які підтверджують достовірність отриманих розрахункових даних.

Ключові слова: акустична хвиля, рівняння Кристоффеля, знесення акустичної хвилі.